

The Conversion of Methane to Methanol: A Reaction Catalyzed by I^+ or I_2^+ ?

Gustavo E. Davico*

Department of Chemistry, University of Idaho, Moscow, Idaho 83844-2343

Received: January 4, 2005; In Final Form: February 17, 2005

The gas-phase reactions of I^+ and I_2^+ with methane were studied to determine which species is involved in the oxidation of methane to methyl sulfate, an intermediate in the production of methanol. We found that while I^+ reacts readily with methane, I_2^+ does not react in our experimental reaction conditions. Reaction products and rate constants are measured and reported. In addition, ab initio calculations were carried out to further understand the reaction mechanism. A revised mechanism of catalysis is proposed which is in excellent agreement with available experimental data and our theoretical computations.

Introduction

The conversion of methane to methanol in high yields and using mild reaction conditions is a very important process of great interest in the petroleum industry. Methanol is much easier and safer to store and transport than methane and can be used as an additive in gasoline as a source of oxygen for cleaner combustion. In a broader perspective this reaction can be classified as a C–H bond activation reaction in hydrocarbons, which is the focus of extensive research for the functionalization of hydrocarbons to value-added organic compounds. A simple yet effective and selective reaction using mild reaction conditions is probably one of the most wanted reactions in organic chemistry. This type of reaction is usually catalyzed by transition metals; platinum compounds are probably the most popular and effective catalysts.¹ However, there are several drawbacks to the use of these catalysts. In addition to their high cost, there are environmental concerns regarding the use of these metal catalysts, and usually the reactions require high temperatures. Therefore, the development of an effective and selective catalyst requiring mild reaction conditions is greatly needed.

There are a large number of different processes reported for this conversion; however, probably one of the most promising is to carry out this oxidation in sulfuric acid or oleum. Periana et al. have extensively studied several transition-metal ions in searching for an effective catalyst for the conversion of methane into methanol in oleum.² Recently they found that some iodine salts catalyzed the conversion of methane to methyl bisulfate, which is then easily converted to methanol.^{3,4} The reaction proceeded in very high yields and at low temperatures. On the basis of the type of iodine salt used in the experiments, these authors concluded that either I^+ or I_2^+ was the catalyst and ruled out I_3^+ and I_4^+ ; however, it appears that they favored I_2^+ as the catalyst on the basis of the results of experiments in which I_2^+ precursors were used. The proposed reaction mechanism³ is shown in Figure 1.

More recently Gang et al. studied the kinetics of this reaction.⁵ They not only confirmed earlier results, but also found that the reaction is catalyzed by a variety of iodine salts and proposed that for all reactions the catalyst, which is formed in the reaction mixture, is the same regardless of the nature of the precursor salt.

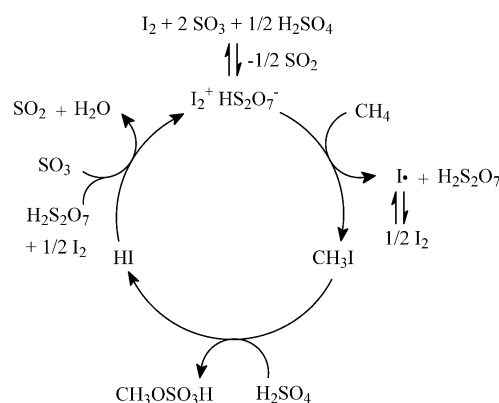


Figure 1. Proposed mechanism of the catalytic conversion of methane to methyl bisulfate by iodine cations.

In this paper we report gas-phase results suggesting that the catalyst in the activation of the C–H bond in methane is I^+ and not I_2^+ . In addition, we also report ab initio calculations that support our experimental results and provide insight into the reaction mechanism. On the basis of these results, we propose an alternative mechanism for the transformation of methane to methyl sulfate.

Experimental Section

The reactions of I^+ and I_2^+ with methane were carried out in a flowing afterglow instrument.^{6,7} Details on the flowing afterglow technique are widely available in the literature, and only a brief summary, emphasizing some unique characteristics of our instrument, is reported here. Our instrument is furnished with Extrel high-transmission, 19 mm diameter rods that allow us to scan m/z values up to 1000 amu with better-than-unit resolution over the entire mass range. Mass scanning is accomplished by using the Merlin data system (Extrel), and rate constants are measured by following the disappearance of the reactant ion as the neutral reactant is injected into one of seven inlets along the flow tube, using pseudo-first-order conditions. The process is automated using custom software written using Labview. Several reaction variables are also required to be measured in the determination of the rate constants, and probably the two most crucial are the reaction tube pressure and the He buffer gas flow. A highly accurate pressure transducer (0.05% of the reading, MKS model 690A) is used to measure the

* E-mail: davico@uidaho.edu

TABLE 1: Product Distributions and Rate Constants for Known Reactions

reaction	product ^a	rate ^b	
		this work ^c	lit. ^d
$\text{N}_2^+ + \text{CH}_3\text{OH}$	$\text{CH}_3\text{OH}^+ (0.15)$	14.1 ± 0.5	$14.0 \pm 30\%^d$
	$\text{CH}_2\text{OH}^+ (0.45)$		14.1 ± 2.9^e
	$\text{HCO}^+ (\text{N}_2\text{H}^+) (0.30)$		
	$\text{CH}_3^+ (0.10)$		
$\text{N}_2^+ + \text{O}_2$	O_2^+	0.77 ± 0.02	$0.50 \pm 15\%^d$ 1.18 ± 0.38^e
$\text{N}_2^+ + \text{CH}_3\text{CN}$	$\text{CH}_3\text{CN}^+ (0.60)$	17.2 ± 1.0	$21.0 \pm 30\%^d$
	$\text{CH}_2\text{CN}^+ (0.40)$		16.8 ± 1.3^e

^a Branching ratios in parentheses. ^b Units of $10^{-10} \text{ cm}^3 \text{ molecule}^{-1} \text{ s}^{-1}$. ^c Rate constants are the average of at least three determinations, and the error bars are 1 standard deviation. ^d Reference 15. ^e Reference 16.

reaction tube pressure, while the helium flow is measured using a digital mass flow controller with an accuracy of 1% of the measured flow (MKS model 179A).

Iodine cations were formed by electron impact on vaporized iodine (Fisher Scientific, ACS grade) and allowed to react with methane (99.97%). Changing the ionization conditions yielded I^+ or I_2^+ as the major product. A typical spectrum and sample kinetic data are included in the Supporting Information.

Computations were carried out using the Gaussian 98 suite of programs.⁸ For carbon and oxygen the cc-pVDZ basis set^{9,10} was used, whereas for iodine the LanL2DZ effective core potential^{11–13} (ECP) was used, supplemented with polarization and diffuse functions as proposed by Radom et al.¹⁴ This ECP includes relativistic effects in the core electrons. Geometries were optimized at the MP2 level followed by calculation of the force constants to determine the ZPVE (not scaled) and to determine the nature of the stationary point, minimum, or transition state. Single-point calculations at the CCSD(T) level were performed using the same basis set for iodine and the cc-pVTZ basis set for carbon and hydrogen atoms. IRC calculations at the MP2 level were performed for all transition structures to ensure they connect the reported minima.

Instrument Validation

Since this is our first study using this instrument, we measured the kinetics of a few reactions for which the reaction rates are very well-known for calibration purposes. The reactions are listed in Table 1 and include dissociative and nondissociative charge-transfer reactions measured at 298 K.

The reaction rates span a range of 2 orders of magnitude from 10^{-9} to $10^{-11} \text{ cm}^3 \text{ molecule}^{-1} \text{ s}^{-1}$ and are in perfect agreement with accepted values¹⁵ and recently published figures.¹⁶ The rates for the reactions of N_2^+ with methanol and acetonitrile fall between the error bars of the published values, whereas in the reaction with oxygen our result falls between those reported in the literature, and the error bars almost overlap with the recent value reported by Hadad et al.¹⁶ There is substantially more variability in the ionic branching ratios for these reactions reported in the literature; however, our results are in general agreement with published data with one exception: the observation of the peak at m/z 29 amu in the reaction of N_2^+ with CH_3OH (1 mass unit above the parent ion, N_2^+). This ion could be either HCO^+ or N_2H^+ , since both channels seem to be exothermic. If N_2 , H_2 , and H are assumed to be the neutral species in the reaction channel producing HCO^+ , then this reaction is exothermic by about 61.5 kcal/mol.¹⁷ A similar value, -61.9 kcal/mol , is estimated for the production of $\text{N}_2\text{H}^+ + \text{CH}_2\text{OH}$ through a simple hydrogen transfer reaction. (The heat of

TABLE 2: Product Distributions and Rate Constants for the Reaction of I^+ with Methane

reaction	product ^a	rate ^b	
		this work	lit. ^c
$\text{I}^+ + \text{CH}_4$	$\text{CH}_4\text{I}^+ (0.40)$ $\text{CH}_2\text{I}^+ [\text{H}_2] (0.60)$	$1.61 \pm 0.10 (0.16)$	<1.87
$\text{I}_2^+ + \text{CH}_4$	NR	NR	

^a Expected neutral product in brackets and branching ratios (extrapolated to zero flow) in parentheses. ^b Units of $10^{-10} \text{ cm}^3 \text{ molecule}^{-1} \text{ s}^{-1}$ measured at 298 K. The value in parentheses is the reaction efficiency, k/k_{col} , where the collision rate constant (k_{col}) is calculated using the parametrized trajectory collision rate theory, ref 18. ^c From ref 19.

TABLE 3: Theoretical and Experimental Energies in the Reaction of $\text{I}_2^+ + \text{CH}_4$

compd	energy ^a		compd	energy ^a	
	ab initio ^b	exptl ^c		ab initio ^b	exptl ^c
$\text{CH}_4 + \text{I}_2^+$	0.00		$\text{CH}_3\text{I} + \text{HI}^+$	30.76	37.16
$\text{CH}_3\text{I}^+ + \text{HI}$	10.99	18.10	$\text{CH}_4\text{I}^+ [\text{1a(S)}] + \text{I}$	44.56	
$\text{CH}_2\text{I}_2^+ + \text{H}_2$	29.53	34.64	$\text{CH}_4^+ + \text{I}_2$	81.10	76.2

^a In kcal/mol. ^b Relative energy with respect to the reactants at the CCSD(T)/cc-pVDZ-DZ+//MP2/cc-pVDZ-DZ+ level, including the MP2/cc-pVDZ-DZ+ level ZPVE (see the text for details on the basis set used). ^c Experimental reaction enthalpy, from ref 17.

formation of N_2H^+ is not known experimentally and was estimated computationally by using the reaction $\text{N}_2^+ + \text{H}_2 \rightarrow \text{N}_2\text{H}^+ + \text{H}$ at the MP2/cc-pVDZ level.) Determining the nature of the peak at m/z 29 (HCO^+ , N_2H^+ , or a mixture of both) would require the use of a ^{15}N -labeled N_2 precursor and is beyond the scope of this paper.

Results and Discussion

The experimental results for the reactions of I^+ and I_2^+ with methane are shown in Table 2. The data presented in Table 2 show clearly that I_2^+ does not react with CH_4 at a measurable rate, and therefore, the rate constant for this reaction should be $<5 \times 10^{-13} \text{ cm}^3 \text{ molecule}^{-1} \text{ s}^{-1}$. Depletion of the I_2^+ signal was not observed even at very high flows of CH_4 , which suggests that the rate constant might be substantially lower than that.²⁰ These results are in excellent agreement with theoretical and experimental values on the reaction energies presented in Table 3 (see also the Supporting Information). All reasonable products in the reaction of I_2^+ with methane are not energetically accessible. In addition, the adduct CH_4I_2^+ is predicted to be bound by only 1.7 kcal/mol with respect to reactants at the CCSD(T)/cc-pVDZ-DZ+//MP2/cc-pVDZ-DZ+ level (including ZPVE; see the Supporting Information), which explains why it is not observed even when a high excess of methane is introduced into the flow tube.

In contrast, I^+ reacts with CH_4 at a measurable rate. Mayhew et al.¹⁹ studied the reaction of X^+ ($\text{X} = \text{F}, \text{Cl}, \text{Br}, \text{and I}$) with several compounds, including CH_4 . In their survey they estimate an upper limit for the bimolecular rate constant, $<0.58 \times 10^{-10} \text{ cm}^3 \text{ molecule}^{-1} \text{ s}^{-1}$, presumably by subtracting the termolecular product by using the branching ratio data (see below). After this correction the overall rate obtained in our experiments is in good agreement with their value (see Table 2). The efficiency of the reaction can be calculated as the ratio between the experimental rate constant and the collision rate constant as obtained by using the parametrized trajectory collision rate theory.¹⁸ The reaction is relatively efficient (16%) considering that the reaction has to proceed through a singlet–triplet curve

TABLE 4: Theoretical and Experimental Energies for the Stationary Points in the Reaction of $I^+ + CH_4$

compd	sym ^a	N_{imag}^b	energy	
			ab initio ^c	exptl ^d
$I^+ (^3P_2)$				0
$I^+ (^3P_1)$				20.26
$I^+ (^3P_0)$				18.44
$I^+ (^1D_2)$				39.25
$CH_4 + I^+ (^1D_2)$			29.03	
$CH_4 + I^+ (^3P_2)$			0.00	
1a(S)	C_s	0	-16.51	
1b(S)	C_s	0	-49.02	
1c(S)	C_s	0	-11.79	
1d(S)	C_s	1	-4.19	
1e(S)	C_s	1	-4.58	
1f(S)	C_{4v}	2	-2.57	
1g(S)	C_{3v}	2	-3.49	
1Tsab(S)	C_s	1	-17.14	
1TSbb(S)	C_s	1	-48.57	
1TSbc(S)	C_s	1	0.24	
1a(T)	C_1	0	-6.00	
1TS(T)	C_1	1	30.73	
$CH_2I^+ + H_2$			-11.51	
$CH_3^+ + IH$			15.30	19.43
$CH_3I^+ + H$			24.99	26.89
$^3CH_2I^+ + H_2$			29.11	
$CH_3 + IH^+$			29.44	31.54
$CH_4^+ + I$				49.78
$CH_3I + H^+$				120.47

^a Symmetry point group. ^b Number of imaginary frequencies. ^c Relative energy with respect to the reactants at their ground state at the CCSD(T)/cc-pVDZ-DZ+//MP2/cc-pVDZ-DZ+ level, including the MP2/cc-pVDZ-DZ+ level ZPVE (see the text for details on the basis set used), in kcal/mol. ^d Experimental reaction enthalpy, from ref 17. Energy levels for singly ionized atoms from the *NIST Handbook of Basic Atomic Spectroscopic Data*, ref 21, in kcal/mol.

crossing, since the ground state of I^+ is a triplet state (3P_2)²¹ and the products have singlet spin multiplicity (see below).

Two ionic reaction products were observed, the adduct CH_4I^+ and CH_2I^+ (adduct $-H_2$) in 40% and 60% ratios, respectively. The adduct is presumably a relatively stable structure that is stabilized by collisions with the helium buffer gas before dissociating back to reactants or proceeding to products. The reaction product CH_2I^+ involves an addition and elimination of H_2 that is typical in the reaction of transition-metal cations with hydrocarbons.²² It has also been observed with other electrophiles, such as in the reaction of BH_2^+ with CH_4 and C_2H_6 .^{23,24} In addition to CH_2I^+ , Mayhew et al. also observed CH_3I^+ although with a small branching ratio (14%).¹⁹ We do not observe this reaction channel unless the helium flow in the reaction flow tube is reduced considerably; only under these conditions is a small but noticeable peak corresponding to CH_3I^+ observed. This observation suggests that this reaction channel might be associated with an excited state of I^+ , which remains unquenched in the flow tube at low pressure.

As mentioned before, the ground state of I^+ is a triplet state. As opposed to the other halogens, the two excited spin-orbit states (3P_0 and 3P_1) are well above the ground 3P_2 state, as shown in Table 4. The next excited state is the first excited singlet state 1D_2 . If the ions are completely thermalized, the population of even the first spin-orbit excited state would be negligible at room temperature. We also included in Table 4 the experimental heats of reaction for several different reaction channels in the reaction of $I^+ + CH_4$. All the reaction channels examined are endothermic considering the ground state of I^+ , except for the $CH_2I^+ + H_2$ channel. The heat of reaction for this channel could not be obtained due to the unknown experimental heat of formation of CH_2I^+ , which is the only product we observe

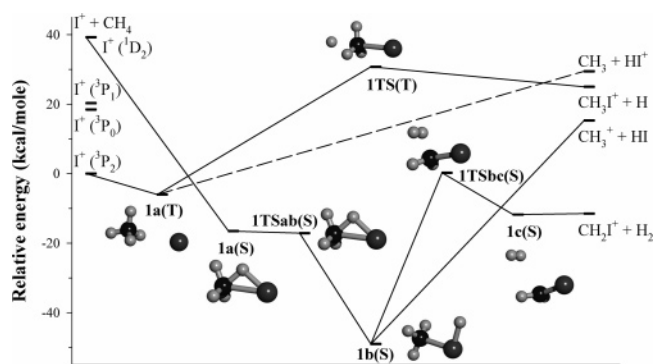


Figure 2. Potential energy surface for the reaction of $I^+ + CH_4$ at the CCSD(T)/cc-pVDZ-DZ+//MP2/cc-pVDZ-DZ+ level, including the MP2/cc-pVDZ-DZ+ level ZPVE (see the text for details on the basis set used). Dashed lines represent dissociation limits.

in our experiments. The data also show clearly that the channel leading to CH_3I^+ is very endothermic; it is even endothermic for the spin-orbit excited states of I^+ . The postulation of the excited electronic 1D_2 state of I^+ in the flow tube is necessary to make this reaction channel exothermic. This can only occur if at least some of the I^+ ions are formed in this excited state in the particular conditions used in the ionizer and/or are not efficiently thermalized, which is promoted at low helium pressure. This seems to be consistent with our results showing a small peak in the mass spectrum at m/z 142 amu when the helium buffer gas flow is decreased substantially. In other words, at lower pressures relaxation and deactivation of excited electronic states are not as efficient, and reaction channels to other products can be opened from those excited states, which otherwise would be endothermic. In the high-pressure limit or in the liquid state this deactivation process would be much more efficient and I^+ would be essentially in its ground state. In addition, other ionic products are also endothermic, including the formation of CH_3^+ (hydride transfer), HI^+ (hydrogen transfer), and CH_4^+ (charge transfer).

Ab initio computations were carried out to obtain more details on the reaction mechanism and thermochemistry. The results are also shown in Table 4. The thermochemical values for the different reaction channels are in very good agreement with theory, considering the assumptions in treating iodine. The values show agreement with experimental data to within 2 kcal/mol, which is approximately the magnitude of the error bars in the experimental values, with the exception of $CH_3^+ + HI$, where the difference is about 4 kcal/mol. Therefore, it is likely that the heat of reaction to form $CH_2I^+ + H_2$ is also predicted reasonably well by this theoretical method. As shown in Table 4, these products are predicted to be the only exothermic channel in the reaction, in perfect agreement with our experiments. It is interesting to note that the experimentally observed peak corresponding to CH_2I^+ must correspond to this structure in its singlet state since the triplet spin state structure is endothermic by around 29 kcal/mol and, therefore, a spin-forbidden reaction pathway is inevitable.

The potential energy surfaces for the singlet and triplet spin states calculated for this reaction are plotted in Figure 2, which also includes the structures for the most relevant stationary points. On the triplet surface an adduct (**1a(T)**) is formed first, which is slightly bound, and its structure resembles a typical ion-dipole complex. On this surface, dissociation to $CH_3I^+ + H$ is not only endothermic, as discussed above, but also kinetically disfavored since transition state **1TS(T)** is around 31 kcal/mol above the reactants. It is interesting to note that the structure of **1TS(T)** suggests that this process occurs through

a back attack similar to those observed in substitution reactions. The asymptote for dissociation of **1a(T)** into $\text{CH}_3 + \text{HI}^+$ is also shown in Figure 2; however, computation of the mechanism for this process was not attempted since it is unlikely to occur due to its endothermicity. Therefore, it is clear that the triplet surface will not lead to any product, and dissociation back to the reactants is favored. However, a singlet–triplet crossing can occur around the flat area surrounding **1a(T)**. Spin changes seem to be relatively efficient in systems containing heavy atoms. As one would expect from relativistic effects, the intersystem crossing is enhanced in systems containing heavy atoms with substantial spin–orbit coupling, as in iodine. A recent report on the reaction of $\text{Re}^+ + \text{CH}_4$ proposes three spin changes while the reaction is still very efficient.²⁵

On the singlet surface adduct **1a(S)** is formed by electrophilic attack into one of the C–H bonds in methane. This adduct is a stationary point at the MP2 level but becomes unbound with respect to **1TSab(S)** at the CCSD(T) level. Obviously the insertion of I^+ into the C–H bond occurs readily, a process that is also generally observed in the electrophilic attack of transition-metal cations on hydrocarbons. Structure **1b(S)** is also the lowest energy structure on the potential energy surface. From this structure, direct dissociation to $\text{CH}_3^+ + \text{HI}$ could occur; however, this process is endothermic. Dissociation to the only exothermic products $\text{CH}_2\text{I}^+ + \text{H}_2$ can occur through **1TSbc(S)** and **1c(S)**. We believe that the modest reaction efficiency observed experimentally is not due to an inefficient singlet–triplet surface crossing but to the fact that after the crossing occurs transition state **1TSbc(S)** is close in energy to the reactants in their ground states. In other words, surmounting this transition state would be the overall reaction-rate-limiting step. In this scenario it is likely that the system could access the singlet–triplet crossing multiple times and dissociate back to the reactants from **1b(S)**. A closer examination of the structures included in Figure 2 shows that, after the insertion into the C–H σ bond in methane and formation of **1b(S)**, a process exothermic by about 51 kcal/mol, a shift of the hydrogen atom back to the carbon atom occurs. This hydrogen atom, together with another hydrogen atom from the methyl group is then readily eliminated as H_2 .

Other structures where all four hydrogen and the iodine atoms are bonded to carbon are found to be transition states or second-order saddle points. These are compounds **1d(S)**, **1e(S)**, **1f(S)**, and **1g(S)**. As can be seen in Table 4, these structures are slightly lower in energy than the reactants. However, they would be relevant only in isotopic label experiments since they acknowledge the scrambling of all four hydrogen atoms in **1b(S)**. In addition, it is interesting to note that these structures are related to those proposed for the very fluxional CH_5^+ system.²⁶

In the high-pressure limit or in a liquid state, structure **1b(S)** would be rapidly stabilized by releasing the excess energy to the surrounding solvent molecules, and the system would be trapped in this potential well.

On the basis of these new results and the mechanism of oxidation of methane proposed by Periana et al.,³ we can now propose an updated mechanism for this reaction. The proposed mechanism, which involves I^+ and not I_2^+ as the catalyst, is shown in Figure 3.

This new mechanism is also in agreement with recent results reported by Gang et al.⁵ They found that the reaction is catalyzed by a variety of iodine salts and suggest that a unique and common species is generated in the reaction conditions, regardless of the precursor salt used. In the same paper, the kinetics of the reaction is reported, and the reaction rate is found to be

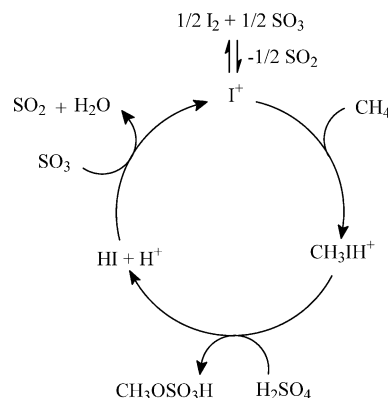


Figure 3. Proposed mechanism for the electrophilic activation of the C–H bond in methane catalyzed by I^+ in oleum.

proportional to the square root of the concentration of I_2 when this compound is used as a precursor, suggesting the formation of an intermediate containing only one iodine atom, in excellent agreement with our results. It is interesting to mention that although stronger oxidation conditions would promote an increment of the I^+ concentration produced from iodine or iodine salts in the oleum reaction mixture, it would probably not affect the reaction appreciably, since I^+ is only required in catalytic amounts.

After the C–H bond activation, H_2SO_4 or any other mild nucleophile in the reaction mixture could react with CH_3IH^+ (or its conjugated base CH_3I) to yield methyl bisulfate through a displacement reaction. One would anticipate that the IH group in CH_3IH^+ would be, in principle, an excellent leaving group for the displacement reaction. The rest of the mechanism, the regeneration of I^+ , is similar to that proposed before.³

Conclusions

In summary, we have found that I^+ reacts readily with methane. The electrophilic attack occurs with the insertion of I^+ into one of the C–H bonds in methane. In contrast, we found that I_2^+ does not react with methane in our reaction conditions. These results prompt us to propose that the active catalyst in the oxidation of methane to methyl bisulfate is I^+ and not I_2^+ , in contrast with an earlier report.³ Our results are also in perfect agreement with available kinetic data and our own ab initio computations. It will be very interesting to determine if I^+ also activates the C–H bond in other hydrocarbons and to find its selectivity with respect to the competing C–C bond activation process. In addition, one would expect that other halogen cations such as Br^+ and Cl^+ would be more electrophilic than I^+ and, therefore, more reactive. Experiments involving the reactions of these cations with methane and ethane are being carried out in our laboratory, and the results will be submitted for publication soon.

Acknowledgment. This work was supported by the University of Idaho, the Idaho NSF-EPSCoR, and the Research Corp. through a Research Innovation Award.

Supporting Information Available: Typical spectrum and raw kinetic data obtained in the reaction of I^+ with CH_4 , including typical experimental conditions, Cartesian coordinates, energies, vibrational frequencies, and structures for intermediates in this reaction, and tables containing computational data on the reactants, products and intermediates for the title reaction (PDF, DOC). This material is available free of charge via the Internet at <http://pubs.acs.org>.

References and Notes

- (1) Periana, R. A.; Taube, D. J.; Gamble, S.; Taube, H.; Satoh, T.; Fujii, H. *Science* **1998**, *280*, 560.
- (2) Periana, R. A.; Bhalla, G.; Tenn, W. J.; Young, K. J. H.; Liu, X. Y.; Mironov, O.; Jones, C.; Ziatdinov, V. R. *J. Mol. Catal. A* **2004**, *220*, 7.
- (3) Periana, R. A.; Mirinov, O.; Taube, D. J.; Gamble, S. *Chem. Commun.* **2002**, 2376.
- (4) Bjerrum, N. J.; Xiao, G.; Hjuler, H. A. U.S. Patent 6,380,444, 2002.
- (5) Gang, X.; Zhu, Y.; Birch, H.; Hjuler, H. A.; Bjerrum, N. J. *Appl. Catal., A* **2004**, *261*, 91.
- (6) Ferguson, E. E.; Fehsenfeld, F. C.; Schmeltekopf, A. L. *Adv. At. Mol. Phys.* **1969**, *5*, 1.
- (7) Bierbaum, V. M.; DePuy, C. H.; Shapiro, R. H.; Stewart, J. H. J. *Am. Chem. Soc.* **1976**, *98*, 4229.
- (8) Frisch, M. J.; Trucks, G. W.; Schlegel, H. B.; Scuseria, G. E.; Robb, M. A.; Cheeseman, J. R.; Zakrzewski, V. G.; Montgomery, J. A.; Stratmann, R. E.; Burant, J. C.; Dapprich, S.; Millam, J. M.; Daniels, A. D.; Kudin, K. N.; Strain, M. C.; Farkas, O.; Tomasi, J.; Barone, V.; Cossi, M.; Cammi, R.; Mennucci, B.; Pomelli, C.; Adamo, C.; Clifford, S.; Ochterski, J.; Petersson, G. A.; Ayala, P. Y.; Cui, Q.; Morokuma, K.; Malick, D. K.; Rabuck, A. D.; Raghavachari, K.; Foresman, J. V.; Cioslowski, J.; Ortiz, J. V.; Baboul, A. G.; Stefanov, B. B.; Liu, G.; Liashenko, A.; Piskorz, P.; Komaromi, I.; Gomperts, R.; Martin, R. L.; Fox, D. J.; Keith, T.; Al-Laham, M. A.; Peng, C. Y.; Nanayakkara, A.; Gonzales, C.; Challacombe, M.; Gill, P. M. W.; Johnson, B.; Chen, W.; Wong, M. W.; Andres, J. L.; Head-Gordon, M.; Replogle, E. S.; Pople, J. A. *Gaussian 98*, Revision A.9; Gaussian, Inc.: Pittsburgh, PA, 1998.
- (9) Dunning, T. H., Jr. *J. Chem. Phys.* **1989**, *90*, 1007.
- (10) Woon, D. E.; Dunning, T. H., Jr. *J. Chem. Phys.* **1993**, *98*, 1358.
- (11) Hay, P. J.; Wadt, W. R. *J. Chem. Phys.* **1985**, *82*, 270.
- (12) Wadt, W. R.; Hay, P. J. *J. Chem. Phys.* **1985**, *82*, 284.
- (13) Hay, P. J.; Wadt, W. R. *J. Chem. Phys.* **1985**, *82*, 299.
- (14) Glukhovtsev, M. N.; Pross, A.; Radom, L. *J. Am. Chem. Soc.* **1995**, *117*, 2024.
- (15) Anicich, V. G. *J. Phys. Chem. Ref. Data* **1993**, *22*, 1469.
- (16) Cohen, M. H.; Barckholtz, C.; Frink, B. T.; Bond, J. J.; Geise, C. M.; Hoff, J.; Herlinger, J.; Hickey, T.; Hadad, C. M. *J. Phys. Chem. A* **2000**, *104*, 11318.
- (17) Unless otherwise specified, all thermochemical data have been taken or derived from Linstrom, P. J.; Mallard, W. G. *NIST Chemistry WebBook*; NIST Standard Reference Database Number 69; National Institute of Standards and Technology: Gaithersburg, MD, 2003 (<http://webbook.nist.gov>).
- (18) Su, T.; Chesnavich, W. J. *J. Chem. Phys.* **1982**, *76*, 5183.
- (19) Mayhew, C. A.; Smith, D. *Int. J. Mass Spectrom. Ion Processes* **1990**, *100*, 737.
- (20) We have measured rate constants with our instrument down to $1 \times 10^{-12} \text{ cm}^3 \text{ molecule}^{-1} \text{ s}^{-1}$ so far and we have room to go below this value. Analysis of the kinetic data suggests that we could measure rates about 5 times slower. However, in these conditions one has to be careful with the role of impurities in the neutral gas. In addition, it is possible to increase the neutral flow rate by about an order of magnitude and follow the intensity of the parent ion peak. Although this experiment will not yield a useful rate constant, it can be used to estimate if the reaction rate is close to the lowest measurable rate, provided that the impurities in the neutral do not react, which is the case in this reaction. This approach, using a similar instrument (*J. Phys. Chem.* **1989**, *93*, 1130), produced an upper value for the rate constant of chloride ion with methyl chloride of $<2 \times 10^{-13} \text{ cm}^3 \text{ molecule}^{-1} \text{ s}^{-1}$.
- (21) Sansonetti, J. E.; Martin, W. C.; Young, S. L. *Handbook of Basic Atomic Spectroscopic Data*, version 1.1; National Institute of Standards and Technology: Gaithersburg, MD, 2004 (<http://physics.nist.gov/Handbook>).
- (22) Armentrout, P. B. *Top. Organomet. Chem.* **1999**, *4*, 1.
- (23) DePuy, C. H.; Gareyev, R.; Hankin, J.; Davico, G. E.; Krempp, M.; Damrauer, R. *J. Am. Chem. Soc.* **1998**, *120*, 5086.
- (24) Zeng, X.; Davico, G. E. *J. Phys. Chem. A* **2003**, *107*, 11565.
- (25) Armentrout, M. M.; Li, F.-X.; Armentrout, P. B. *J. Phys. Chem. A* **2004**, *108*, 9660.
- (26) Schreiner, P. R. *Angew. Chem., Int. Ed.* **2000**, *39*, 3239.